Preparation and magnetical studies of $Mn_{50}Al_{50}$/Al bilayer films

P. C. Kuo
Institute of Materials Science and Engineering, National Taiwan University, Taipei 107, Taiwan

Y. D. Yao
Institute of Physics, Academia Sinica, Taipei 115, Taiwan

W. R. Chen and J. H. Huang
Institute of Materials Science and Engineering, National Taiwan University, Taipei 107, Taiwan

$Mn_{50}Al_{50}$/Al bilayer films were fabricated on a glass substrate by rf magnetron sputtering. The films were subsequently heat-treated in order to transform nonmagnetic MnAl ϵ-phase to magnetic τ-phase. The addition of Al buffer layer could enhance the adhesion of the MnAl films, and for $Mn_{50}Al_{50}$/Al bilayer films with Al layer thickness between 5 and 15 nm, we can obtain high saturation magnetization ($>$390 emu/cm^3), and high coercivity ($>$2200 Oe) $Mn_{50}Al_{50}$/Al films for practical usage. Bending beam method analysis shows that the larger the residual stress of the $Mn_{50}Al_{50}$/Al bilayer film is, the higher the coercivity is. The relations between the saturation magnetization, the coercivity and the phase transition, the microstructures of the films are discussed. © *1997 American Institute of Physics.* [S0021-8979(97)52208-0]

I. INTRODUCTION

In 1985, Kono[1] found that there is a ferromagnetic τ-phase in the MnAl alloy. After that, the structure and magnetic properties of this τ-phase were extensively investigated.[2–7] This τ-phase contains about 45–58 at. % Mn. It has the CuAu I type structure and exhibits interesting permanent magnetic properties. The mechanism for the formation of the τ-phase is that the high-temperature nonmagnetic ϵ-phase(hcp) transforms into a nonmagnetic ϵ-phase(orthorhombic) by an ordering reaction, then transforms into a ferromagnetic τ-phase(fct) by a martensitic phase transition.[4,8]

Recently, a variety of MnAl thin films have been studied[9–14] due to the progress of thin film techniques in magnetic materials. In previous work,[14] we found that the maximum magnetic properties of MnAl thin films occur at the composition of $Mn_{50}Al_{50}$ after heat-treatment. These films have nearly single phase of ferromagnetic τ-phase. However, because the magnetic τ-phase comes from the martensitic transformation of the ϵ-phase, the adhesion of MnAl film with the glass substrate is poor.

In this article, we study the effect of an Al buffer layer on the adhesion and magnetic properties of $Mn_{50}Al_{50}$ film.

II. EXPERIMENT

The $Mn_{50}Al_{50}$/Al bilayer films were deposited by an rf magnetron sputtering system. The Al films were deposited onto a room-temperature glass substrate and then the MnAl films were deposited on the Al films. A $Mn_{50.4}Al_{49.6}$ alloy target were produced from high purity (99.99%) Mn and Al elements using a high-frequency induction furnace with a protective argon atmosphere. This composition of MnAl alloy target was proved later on to produce very good $Mn_{50}Al_{50}$ alloy films. The compositions of all the MnAl films were determined by electron probe microanalyzer (EPMA). The microstructure of these films were studied by transmission electron microscopy (TEM). The $Mn_{50}Al_{50}$/Al bilayer films with various thickness of Al layer and 600 nm thickness of $Mn_{50}Al_{50}$ layer were used in this study. Thickness of the films were measured by a α-step and SIMS. The rf power was kept at 80 W, distance between target and substrate was set at 45 nm, and the deposition rate was 0.5 nm/s. The base pressure in the system was 5×10^{-7} Torr, and after the high purity Ar gas was introduced, the discharge gas pressure was set at 1 mTorr. After sputtering, the $Mn_{50}Al_{50}$/Al bilayer films were annealed at temperatures between 100 °C and 450 °C in vacuum for 30 min.

Magnetic properties of the films were measured with VSM at room temperature. Crystal structure of the films were characterized by x-ray diffractometer. The stress of MnAl/Al film during annealing is measured by a bending beam method. Under this method, film sample was clamp in the vacuum oven and from the reflection of a He–Ne laser beam, we converted the signal of the deflection position of the laser beam into the stress value continuously. The film-substrate adhesion was determined by a crude scratch test with stainless-steel tweezers.

III. RESULTS AND DISCUSSION

Figure 1 shows the x-ray diffraction patterns of the as-deposited $Mn_{50}Al_{50}$ films with various thickness of Al underlayers. For samples with the thickness of Al underlayer be-

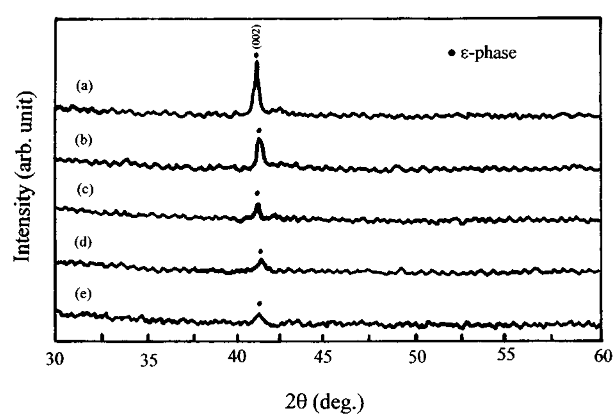

FIG. 1. X-ray diffraction patterns of as deposited $Mn_{50}Al_{50}$ films with thickness of 600 nm, the thickness of Al underlayer are (a) 0 nm, (b) 30 nm, (c) 60 nm, (d) 90 nm, and (e) 120 nm, respectively.

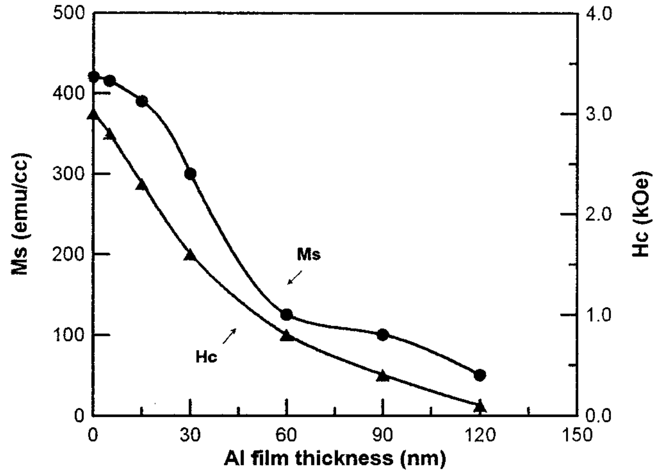

FIG. 2. Magnetic properties of $Mn_{50}Al_{50}$/Al bilayer films with various thickness of Al layer after annealed at 400 °C for 30 min.

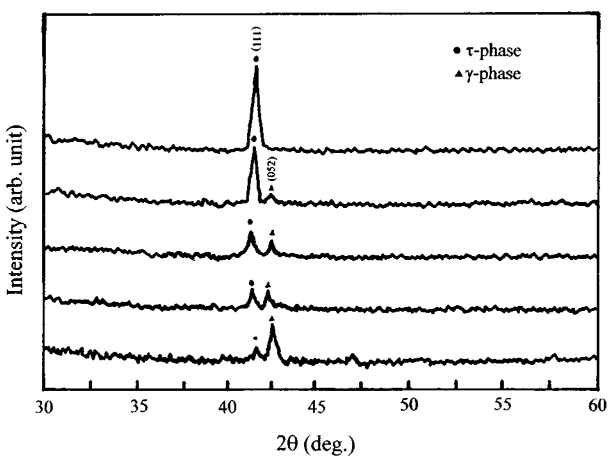

FIG. 3. X-ray diffraction patterns of $Mn_{50}Al_{50}$/Al films after annealed at 400 °C for 30 min, the thickness of Al layers are (a) 0 nm, (b) 30 nm, (c) 60 nm, (d) 90 nm, and (e) 120 nm, respectively.

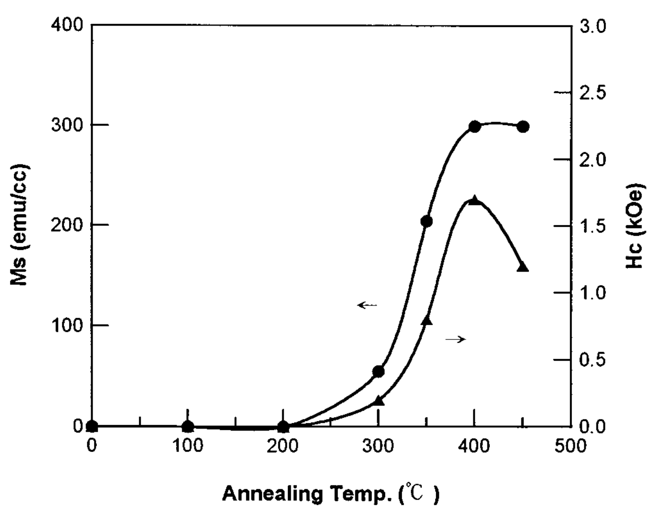

FIG. 4. Annealing temperature dependence of M_s and H_c for $Mn_{50}Al_{50}$/Al bilayer films.

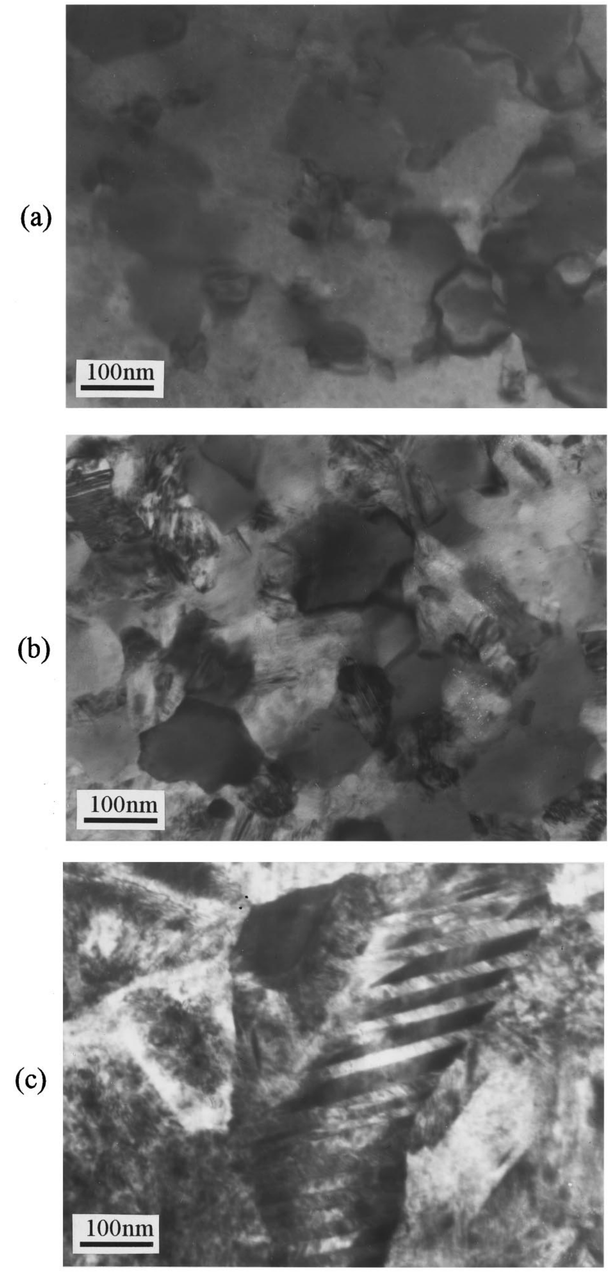

FIG. 5. The TEM photographs of the films annealing at (a) 100 °C, (b) 300 °C, and (c) 400 °C for 30 min.

low 30 nm the diffraction peaks indicated that $Mn_{50}Al_{50}$ films form quite well crystalline ϵ-phase. However, if the Al underlayer becomes thicker than 30 nm, the ϵ-phase seems less well crystallized gradually. Figure 2 shows the saturation magnetization M_s and coercivity H_c of the $Mn_{50}Al_{50}$/Al bilayer films as a function of Al layer thickness. We can see that the M_s and H_c are still quite high, for samples with the Al thickness less than 15 nm. But they decrease quite a lot, when the thickness of Al layer is increased from 15 nm to 120 nm. The decrease of M_s and H_c with increasing Al layer thickness can be attributed to the formation of the nonmagnetic γ-phase after the annealing treatment. This can be seen from the x-ray diffraction patterns of $Mn_{50}Al_{50}$/Al films after annealing at 400 °C for 30 min as shown in Fig. 3. Since the magnetic τ-phase is transformed from ϵ-phase during anneal-

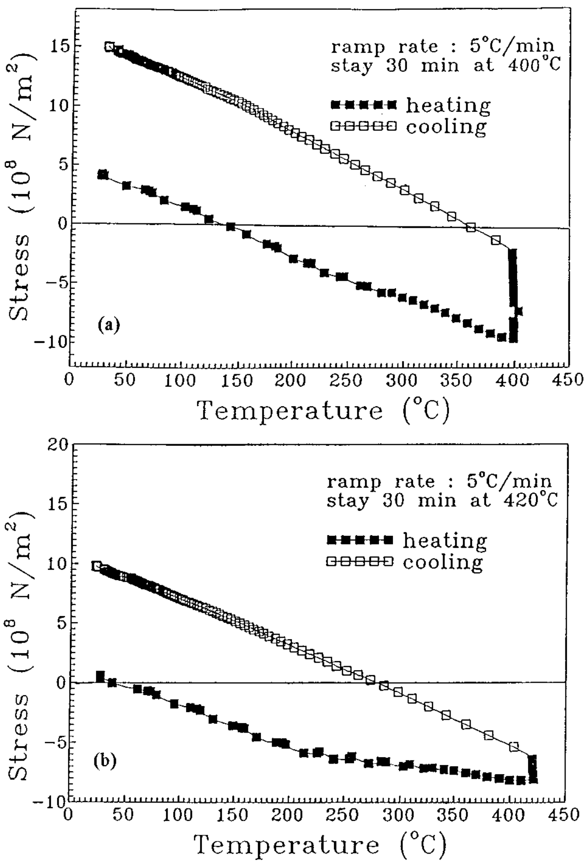

FIG. 6. Temperature dependence of stress for $Mn_{50}Al_{50}$/Al bilayer films, the thickness of Al layer is 30 nm. (a) Annealed at 400 °C for 30 min. (b) Annealed at 420 °C for 30 min.

ing, the decrease of the amount of τ-phase with increasing thickness of Al layer is due to the less amount of ϵ-phase in as-deposited MnAl layer.

Figure 4 shows the magnetic properties of the $Mn_{50}Al_{50}$/Al bilayer films as a function of annealing temperature between 100 °C and 450 °C. The thickness of Al underlayer is 30 nm. It is seen that as the annealing temperature is above 200 °C, the M_s and H_c increase rapidly with increasing annealing temperature. The increase of M_s and H_c with annealing temperature is due to that the amount of τ-phase which is transformed from ϵ-phase is increased with annealing temperature. At 400 °C, the M_s reached its maximum value and remained unchanged with the temperature. This means that the transformation of ϵ-phase to τ-phase is completed at temperatures above 400 °C.

Figures 5(a), 5(b), and 5(c) present the TEM photographs of the films annealing at 100, 300, and 400 °C for 30 min, respectively. The film annealing at 100 °C as shown in Fig. 5(a) is the nonmagnetic ϵ-phase with grain size roughly about 150 nm. Figure 5(b) shows a small amount of platelike τ-phase appears after annealing at 300 °C. In Fig. 5(c), the platelike τ-phase with grain size of roughly 300 nm is formed after annealing at 400 °C. Since the magnetocrystalline anisotropy constant of the τ-phase is as high as 10^7 erg/cm^3,[1] the magnitude of H_c increases with the amount of τ-phase in the film.

Figure 6 shows the temperature dependence of the stress for the bilayer MnAl alloy films annealed with a heating rate of 5 °C/min from room temperature to 400 °C [Fig. 6(a)] and 420 °C [Fig. 6(b)], respectively. At the highest temperature for each case, it was kept isothermally annealing for 30 min, and then furnace-cooled to room temperature. From Fig. 6, we can see that the residual stress of these two samples are about the same ($\sigma \cong -8\times 10^8$ N/m^2) as the temperatures rise to the annealing temperatures (400 °C and 420 °C). However, after 30 min annealing and cooling down to room temperature, the residual tensile stress of the film which annealed at 400 °C ($\sigma = 15\times 10^8$ N/m^2) is larger than that of the film which annealed at 420 °C ($\sigma = 10\times 10^8$ N/m^2). Therefore, the decrease of Hc above 400 °C as shown in Fig. 4 is owing to the decrease of final residual stress in the film as shown in Fig. 6.

Finally, we use stainless-steel tweezers to determined the film-substrate adhesion by a crude scratch test. It is found that the adhesion of all the $Mn_{50}Al_{50}$/Al bilayer films with glass substrate is much better than that of $Mn_{50}Al_{50}$ single layer films, even for the sample with an Al underlayer of 5 nm thickness.

In conclusion, we have reported the effect of an Al buffer layer on the adhesion and the magnetic properties of $Mn_{50}Al_{50}$ films. The Al buffer layer enhances the adhesion between the MnAl films and the glass substrate, and for $Mn_{50}Al_{50}$/Al bilayer films with Al layer thickness between 5 and 15 nm, we can obtain $Mn_{50}Al_{50}$/Al films with high saturation magnetization (>390 emu/cm^3), and high coercivity (>2200 Oe) for practical usage. We have also demonstrated that the saturation magnetization and the coercivity are closely related to the phase transition and the microstructures of the films.

ACKNOWLEDGMENTS

The authors are indebted for the financial support of this work to the National Council of Taiwan under Grant Nos. NSC 85-2216-E-002-017 and NSC 85-2112-M-001-020.

[1] H. Kono, J. Phys. Soc. Jpn. **13**, 1444 (1958).
[2] A. J. J. Koch, P. Hokkeling, M. G. V. D. Streg, and K. J. DeVos, J. Appl. Phys. **31**, 75S (1960).
[3] J. P. Jakubovics and T. W. Jolly, Physica B **86**, 1357 (1976).
[4] J. J. Van Den Brock, H. Donkersloot, G. Van Tendeloo, and J. Van Landuyt, Acta Metall. **27**, 1497 (1979).
[5] J. Van Landuyt, G. Van Tendeloo, J. J. Van Brock, and H. Honkersloot, J. Magn. Magn. Mater. **15–18**, 1451 (1980).
[6] M. A. Bohlmann, J. C. Koo, and J. H. Wise, J. Appl. Phys. **52**, 2542 (1981).
[7] Y. Hara, R. C. O'Handley, and N. J. Grant, J. Magn. Magn. Mater. **54–57**, 1077 (1986).
[8] S. Kohima, T. Ohtani, N. Kato, K. Kojima, Y. Sakamoto, I. Konno, M. Tsukahara, and T. Kubo, AIP Conf. Proc. **24**, 768 (1974).
[9] A. Morisako, M. Matsumoto, and M. Naoe, J. Appl. Phys. **61**, 4281 (1987).
[10] A. Morisako, N. Kohshiro, M. Matsumoto, and M. Naoe, J. Appl. Phys. **67**, 5655 (1990).
[11] J. X. Shen, R. D. Kirby, and D. J. Sellmyer, J. Appl. Phys. **67**, 4929 (1990).
[12] M. Matsumoto, A. Morisako, and J. Ohshima, J. Appl. Phys. **69**, 5172 (1991).
[13] T. L. Cheeks, J. P. Harbison, M. Tanaka, D. M. Hwang, T. Sands, and V. G. Keramidas, J. Appl. Phys. **75**, 6665 (1994).
[14] J. H. Huang, P. C. Kuo, and S. C. Shen, IEEE Trans. Magn. **31**, 2494 (1995).